INHOMOGENEOUS STELLAR MODELS. IV. MODELS WITH CONTINUOUSLY VARYING CHEMICAL COMPOSITION*

R. Härm and M. Schwarzschild
Princeton University Observatory
Received November 3, 1954

ABSTRACT

Nine sample models are constructed in which the mean molecular weight varies from the center to the surface by a factor of 2.5 and in which this variation occurs continuously inside an intermediate zone. These models are compared with simpler models in which the same composition variation occurs discontinuously at an interface. The comparison shows that the simpler, discontinuous models may be used to compute the luminosity with satisfactory accuracy but that they tend to exaggerate the radii—in certain cases by an order of magnitude.

I. INTRODUCTION

In recent investigations about the internal structure of red giants, several series of stellar models have been constructed with inhomogeneities in the chemical composition. In nearly all cases these inhomogeneities were represented by an abrupt change of the composition at one particular place in the stellar interior, so that the models derived consisted of a homogeneous interior and a homogeneous envelope with a discontinuous change in the molecular weight at the interface. On the other hand, in real stars any inhomogeneities would presumably occur without sharp discontinuities. Thus the question arises how far models with continuous variation of composition might differ from those in which the inhomogeneity is limited to one discontinuous jump.

In an attempt to answer this question, nine sample models with continuously varying molecular weight have been constructed. Each of these models consists of three parts—a homogeneous envelope, with the molecular weight μ_e; a homogeneous core, with the molecular weight μ_i; and an intermediate zone in which the molecular weight varies continuously from μ_i at the inner interface to μ_e at the outer interface. For the ratio of μ_i to μ_e, the large value of 2.5 was used here throughout, in order to make the effects looked for as large as possible. Finally, the variation of the composition in the intermediate zone was arbitrarily chosen so that the molecular weight changes proportional to M_r (see eq. [11]). The nine models thus selected are obviously only a feeble sample of all the possible models with continuously varying composition. It is nevertheless hoped that the results obtained with these sample models can be generalized with some assurance.

II. ASSUMPTIONS AND BASIC EQUATIONS

The following simplifying assumptions have been used for the computations: (*a*) The variation of the chemical composition affects only the hydrogen and helium content; the fraction Z of the heavy elements is constant throughout the star. (*b*) The absorption coefficient follows Kramers' law with a constant guillotine factor. (*c*) Radiation pressure and degeneracy are negligible. (*d*) In the first four models, which have convective cores, the entire energy generation occurs within the convective core. (*e*) In the last five models, which have isothermal cores, the entire energy generation occurs within an infinitely thin shell at the boundary of the core.

For the present purpose it does not appear too important whether the foregoing assumptions closely approximate real stars. It will, however, be important that these

* This research was supported in part by funds of the Eugene Higgins Trust allocated to Princeton University and in part by contract with the Office of Naval Research.

models with continuously varying composition be compared only with such discontinuous models as were computed under the same physical assumptions. The computations have been carried out with the help of the following definition and equations:

Nomenclature, equations, etc.

Identical with equations (1)–(9) in Paper I of this series (Oke and Schwarzschild 1952). (1)–(9)

Here, however, $\alpha = 0$ throughout.

Emden variables for isothermal core

$$t = \text{Const.} = t_c\,, \qquad p = e^{-\psi^*} p_c\,, \qquad x = \xi \frac{x_1}{\xi_1}. \tag{10}$$

Composition variation in intermediate zone

$$l = \left(\frac{q}{q_2}\right)^{-\nu}, \qquad j = l^{0.30}. \tag{11}$$

Logarithmic variables for intermediate zone

$$\lambda = \log \frac{p}{p_0}, \qquad \tau = \log \frac{t}{t_0}, \qquad \psi = \log \frac{q}{q_0}, \qquad y = \log \frac{x}{x_0}, \tag{12}$$

with

$$q_2^{\nu} \frac{q_0^{1-\nu}}{x_0 t_0} = 1\,, \qquad q_2^{\nu} \frac{p_0 x_0^3}{q_0^{1+\nu} t_0} = 1, \qquad q_2^{1.3\nu} C \frac{q_0^{-1.3\nu} p_0^2}{x_0 t_0^{9.5}} = 1\,, \qquad x_0 = x_1\,. \tag{13}$$

Basic equations in logarithmic variables

$$\begin{aligned} \log\left(-\frac{d\lambda}{dy}\right) &= -\tau + (1-\nu)\psi - y && [=\log V]\,, \\ \log\left(-\frac{d\tau}{dy}\right) &= +2\lambda - 9.5\tau - 1.3\nu\psi - y && \left[=\log \frac{V}{n+1}\right], \\ \log\left(+\frac{d\psi}{dy}\right) &= +\lambda - \tau - (1+\nu)\psi + 3y && [=\log U]\,. \end{aligned} \tag{14}$$

Fitting condition at outer interface

$$U,\ V,\ \text{and}\ (n+1)\ \text{continuous}\,. \tag{15}$$

Fitting condition at inner interface

For all models: U and V continuous, (16)

For models with isothermal core: no fitting condition for $(n+1)$, (17)

For models with convective core: $(n+1)$ continuous and equal to 2.5 . (18)

The last of the foregoing conditions may be derived as follows: For a layer in which the molecular weight varies with height, one finds, by the usual perturbation arguments, the condition for stability against convection to be

$$\left(-\frac{1}{T}\frac{dT}{dr}\right) < \frac{\gamma-1}{\gamma}\left(-\frac{1}{p}\frac{dP}{dr}\right) + \left(-\frac{1}{\mu}\frac{d\mu}{dr}\right). \tag{19}$$

In the derivation of this condition, it is assumed that the molecular weight of a given element of matter does not vary as a consequence of pressure or temperature variations, an assumption valid in the deep interior. If the molecular weight decreases with height, as is the case in the present models, condition (19) is much less stringent for the temperature gradient then the usual stability condition,

$$\left(-\frac{1}{T}\frac{dT}{dr}\right)<\frac{\gamma-1}{\gamma}\left(-\frac{1}{p}\frac{dP}{dr}\right). \tag{20}$$

This is understandable because the temperature gradient, to cause instability under the conditions here considered, would have to be appreciably steeper than the adiabatic temperature gradient, to overcome the greater average weight of the particles at the bottom of the zone as compared with those at the top of the zone. Nevertheless, it appears unlikely that the fulfilment of the weak condition (19) suffices for stability. If a layer fulfils condition (19) but not the stronger condition (20), one may—assuming energy to be available—introduce a perturbation which, in a given volume element, completely mixes up the material and thus, in this volume element, eliminates the gradient of μ. Now, because equation (20) is not fulfilled, the interior of the element will be unstable against turbulent motions of subelements. This turbulence would presumably eat into the neighboring region and thus eventually turn the entire zone from a layer in radiative equilibrium with a μ-gradient into a layer in convective equilibrium with a constant μ. Hence it appears fairly certain that the usual condition (20) must be fulfilled for stability against convection, even in zones in which the molecular weight decreases with height.

In the particular case here under consideration, the foregoing argument seems very certain. If condition (19) were to be employed in the intermediate zone, so that, at the inner boundary of this zone, just the equal sign would hold in this equation, then the temperature gradient would have to drop at the interface from the value given by this equation to the value given by condition (20) in the convective core. This finite drop of the temperature gradient would produce a finite drop of the radiative flux. To compensate for this drop, the convective flux in the core would have to be finite to the very limit of the core. Up to the core surface, therefore, the turbulence, in Öpik's terms, would be active and hence would be sure to eat into the neighboring intermediate zone, eliminate its μ-gradient by mixing, and thus make the zone unstable. Hence it seems certain that the stronger condition (20) must be fulfilled in the intermediate zone, from which follows the fitting condition (18).

III. CONSTRUCTION OF MODELS

To construct the models here considered, numerical solutions were needed for all three portions—the envelopes, the intermediate zones, and the cores. For the envelopes, the one-parameter family of solutions (characterized by the parameter C) was available, since it had already been used in the preceding papers of this series. Similarly, for the cores, the unique solution for a convective core (for models 1–4) and the unique solution for a nondegenerate isothermal core (for models 5–9) are available in tabular form (Comrie 1932; Wares and Chandrasekhar 1949). Only for the intermediate zone with continuously varying composition, did new numerical integrations have to be computed. These numerical integrations were performed in terms of the logarithmic variables according to definitions (12) with the basic equations (14). For each model, a definite value of ν was arbitrarily chosen which fixed the rate of change of the molecular weight in the intermediate zone according to equation (11).

The numerical integrations for the intermediate zone of each of the first four models were started at the edge of the convective core and at the end were fitted to the inner boundary of the envelope as follows. A trial value was chosen for ξ_1 which represents the termination point of the convective core. At this point the values of U_1 and V_1 were read from the tabulation of the core solution. These two values, together with $(n+1)_1 = 2.5$, give, according to the bracketed expressions in equations (14), three conditions for the four starting values λ_1, τ_1, ψ_1, and y_1. Since, in addition, $y_1 = 0$ according to the last equation (13), all the starting values can be determined from these relations, and a unique solution for every trial value of ξ_1 can be obtained by numerical integration outward. Each integration was terminated when the change in ψ, i.e., in q, corresponded to a change in l, according to equation (11), of exactly a factor of 2.5. Thus such an integration represented a zone in which the molecular weight decreased by a factor of 2.5. At the end-point, sharply defined by this condition, the values of U_2, V_2, and $(n+1)_2$ were read from the integration. These values had to be fitted to the envelope solutions according to condition (15). Since the one-parameter family of envelope solutions covers the U–V plane, one can determine by graphical interpolation the value of $(n+1)$ given by the envelope solutions for the point U_2, V_2, representing the end-point of the intermediate zone integration. In general, the value of $(n+1)$ thus obtained from the envelopes will differ from the value reached at the end of the intermediate zone integration. However, by changing the trial value for ξ_1 and reintegrating, a value of ξ_1 could be determined for each model such that the corresponding integration gave a terminal value of $(n+1)$ in agreement with the value from the envelope solutions for the same U, V point. This completed the fitting of the entire model.

Exactly the same method of integrating and fitting here described for the models with convective cores was also used for the models with isothermal cores, but with one change. According to equation (17), the polytropic index at the start of the intermediate zone at the inner interface is free for models with isothermal cores. This extra freedom arises physically from the circumstance that the core for models with convective cores is determined in size and mass by the equilibrium conditions, whereas for models with isothermal cores the past evolution rather than the equilibrium conditions determines the size of the core. Each model with an isothermal core is then characterized by two arbitrary parameters, for which we may choose ν as before and ξ_1, which gives the termination point of the core. Now $(n+1)_1$ is used as eigen parameter which has to be determined by trial and error to fulfil the fitting conditions at the outer interface.

The characteristics thus obtained are listed in Table 1 for the models with convective cores and in Table 2 for the models with isothermal cores. The cores and intermediate zones of all these models are represented in Figure 1 in terms of the U–V plane.

It may be noted that in all the models here computed the fraction of the mass contained in the core is rather small (q_1 at most 13 per cent) but that the mass fraction contained in the inhomogeneous intermediate zones varies greatly from model to model ($q_2 - q_1$ ranging from 9 to 70 per cent).

IV. COMPARISON WITH DISCONTINUOUS MODELS

The hydrogen content of the present model varies continuously from a high value in the envelope to a low value in the core. These continuous models are to be compared with discontinuous models in which the hydrogen content jumps discontinuously from a high and constant value in the outer parts to a low and constant value in the inner parts. Each continuous model should be compared with a discontinuous model which has the same over-all hydrogen content (the heavy-element content, Z, is here taken constant throughout each model as well as from model to model). It is therefore necessary to compute, first, the over-all or mean hydrogen content, which is given by

$$X_m = \int_0^1 X \, d q \, . \tag{21}$$

The quadrature can be performed for the present continuous models with the help of equations (4) and (11). The result is

$$X_m = X_e - \frac{\nu}{1+\nu} \frac{4}{5} \left(\frac{q_2}{\mu_e} - \frac{q_1}{\mu_i} \right). \tag{22}$$

If we define the over-all mean molecular weight of a star as that mean molecular weight which corresponds to the over-all hydrogen content, we obtain, from equation (22),

$$\frac{\mu_e}{\mu_m} = 1 - \frac{\nu}{1+\nu} \left(q_2 - \frac{\mu_e}{\mu_i} q_1 \right). \tag{23}$$

TABLE 1

CHARACTERISTICS OF MODELS WITH CONVECTIVE CORES

	I	II	III	IV
ν	1.0	0.5	0.4	0.38
ξ_1	1.422	1.319	1.294	1.290
U_1	2.412	2.493	2.511	2.514
V_1	1.764	1.506	1.448	1.436
$(n+1)_1$	2.500	2.500	2.500	2.500
U_2	1.230	1.081	0.687	0.504
V_2	1.378	2.493	3.857	4.561
$(n+1)_2$	3.014	3.572	3.947	4.059
$\log C$	−5.55	−5.18	−4.75	−4.60
$\log x_2$	−0.992	−0.860	−0.729	−0.646
$\log q_2$	−0.815	−0.438	−0.188	−0.114
$\log t_2$	+0.038	+0.025	−0.045	−0.127
$\log p_2$	+2.289	+2.200	+1.791	+1.400
$\log x_1$	−1.244	−1.379	−1.469	−1.487
$\log q_1$	−1.213	−1.234	−1.183	−1.161
$\log t_1$	+0.183	+0.365	+0.524	+0.566
$\log p_1$	+2.688	+3.267	+3.752	+3.870
$\log t_c$	+0.332	+0.493	+0.647	+0.689
$\log p_c$	+3.060	+3.587	+4.060	+4.178
$q_1 = M_1/M$	0.0612	0.0583	0.0656	0.0690
$q_2 = M_2/M$	0.153	0.365	0.649	0.769
q_d	0.107	0.190	0.297	0.340
μ_e/μ_m	0.936	0.886	0.822	0.796

Similarly, for a discontinuous comparison model, in which the composition jump occurs at a mass fraction q_d, the over-all hydrogen content is given by

$$X_m = X_e (1 - q_d) + X_i q_d . \tag{24}$$

If one now equates that over-all hydrogen content of a continuous model as given by equation (22) with that of a discontinuous model as given by equation (24), one obtains

$$q_d = \frac{\nu}{1+\nu} \left(\frac{\mu_i}{\mu_i - \mu_e} q_2 - \frac{\mu_e}{\mu_i - \mu_e} q_1 \right). \tag{25}$$

This relation gives the q_d-value, which a discontinuous comparison model must have, in terms of the characteristics of the continuous model. The values of q_d according to equation (25) and of μ_e/μ_m according to equation (23) for the present nine models are given in the last two lines of Tables 1 and 2.

Discontinuous models with convective cores exactly equivalent to the first four of the present continuous models have been given by Oke and Schwarzschild (1952). Interpolation into their Table 1 according to the q_d-values given at the foot of the present Table 1 (with q_d being equivalent to their q_2) gives exactly the needed comparison models. No discontinuous comparison models were available for the present continuous models with isothermal cores. Therefore, discontinuous comparison models were here computed

TABLE 2

CHARACTERISTICS OF MODELS WITH ISOTHERMAL CORES

	V	VI	VII	VIII	IX
ν	1.0	0.5	0.49	0.50	0.42
ξ_1	9.0	9.0	9.0	25.0	25.0
U_1	1.000	1.000	1.000	0.794	0.795
V_1	2.518	2.517	2.517	2.161	2.161
$(n+1)_1$	3.402	3.510	3.512	3.488	3.506
U_2	0.831	0.310	0.227	0.807	0.444
V_2	1.677	4.182	4.648	2.683	4.038
$(n+1)_2$	3.379	4.111	4.160	3.730	4.051
$\log C$	−5.30	−3.78	−3.66	−4.83	−4.18
$\log x_2$	−1.101	−0.879	−0.769	−0.960	−0.817
$\log q_2$	−0.732	−0.106	−0.068	−0.389	−0.136
$\log t_2$	+0.145	+0.151	+0.033	+0.143	+0.075
$\log p_2$	+2.636	+2.173	+1.628	+2.541	+2.038
$\log x_1$	−1.574	−2.139	−2.145	−1.881	−2.069
$\log q_1$	−1.130	−0.902	−0.880	−1.185	−1.083
$\log t_1$	+0.441	+1.233	+1.262	+0.760	+1.049
$\log p_1$	+3.637	+6.350	+6.420	+4.719	+5.677
$\log t_c$	+0.441	+1.233	+1.262	+0.760	+1.049
$\log p_c$	+5.145	+7.858	+7.928	+7.280	+8.238
$q_1=M_1/M$	0.0741	0.125	0.132	0.0653	0.0826
$q_2=M_2/M$	0.185	0.783	0.855	0.408	0.731
q_d	0.129	0.407	0.440	0.212	0.344
μ_e/μ_m	0.922	0.756	0.736	0.873	0.794

for the rather extreme cases VII and IX of Table 2. The two comparison models were adjusted to models VII and IX, respectively, according to the q_d-values, insuring equality in total hydrogen content, and the q_1-values, insuring equality in the mass fraction contained in the isothermal core.

Among all the characteristics in terms of which the continuous and discontinuous models may be compared, the two most directly related to observations are the luminosity and the radius. The luminosity may be computed from equation (7), which gives

$$L=\left[\frac{4ac}{3}(4\pi)^{3}\left(\frac{HG}{k}\right)^{7}\right]\left[M^{5}\mu_m^{7}\frac{(t/\bar{g})_0}{\kappa_{0m}}T_c^{1/2}\right]\left[\frac{C}{t_c^{1/2}}\left(\frac{\mu_e}{\mu_m}\right)^{7.7}\right]. \tag{26}$$

Here the first bracket contains only universal constants. The second bracket contains the mass and central temperature of the star and its over-all composition, which affects both the mean molecular weight and the constant in the opacity law. The last bracket contains the relevant nondimensional characteristics of the models in which the continuous models may differ from the discontinuous ones. The radius may be computed by applying the second of equations (3) to the center of the star, which gives

$$R=\left[\frac{HG}{k}\right]\left[\frac{M\mu_m}{T_c}\right]\left[t_c\,\frac{\mu_e}{\mu_m}\right]. \tag{27}$$

Here the three brackets have the same characteristics as those in equation (26). The last brackets of equations (26) and (27), which give the dependence of the luminosity and radius on the stellar model, are listed in Table 3 for all the models here considered.

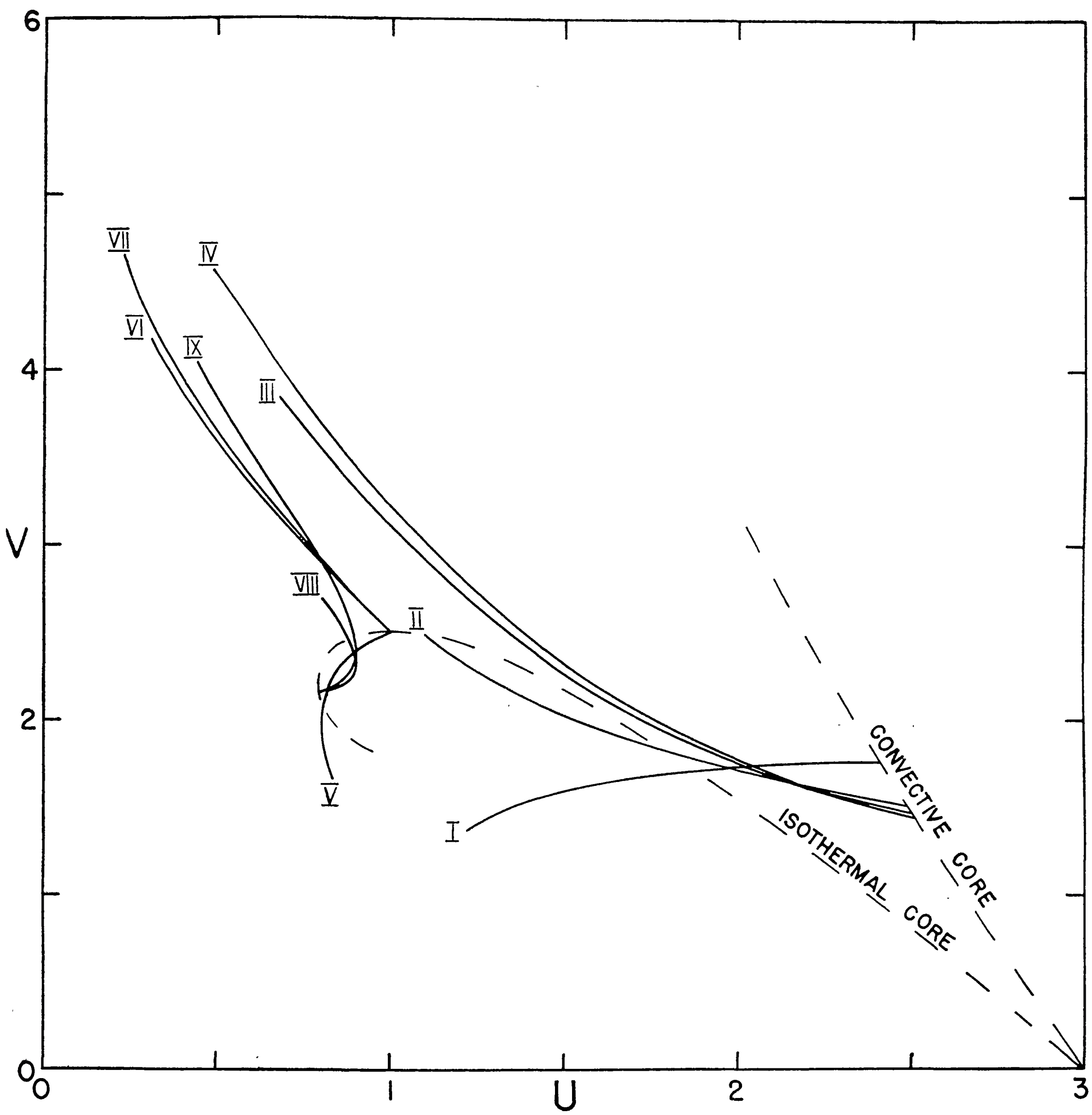

FIG. 1.—Representation of models in terms of the homology invariants U and V. The intermediate zones of models I–IV start at the convective core, those of models V–IX at the isothermal core. The envelopes are not shown.

V. RESULTS

Consider a star of a given mass, central temperature, and over-all chemical composition. The second column of Table 3 gives for such a star substantially the logarithm of the luminosity in its dependence on the model, i.e., on the distribution of the hydrogen content throughout the star. The table shows that the present continuous models differ in luminosity from the equivalent discontinuous models only little. In fact, even the extreme cases IV and VII, in which the variation of the composition is spread over 70 per cent of the stellar mass, differ from the discontinuous models only by 0.11 in the logarithm of the luminosity or 0.28 in bolometric magnitude. We may then conclude that we can compute the luminosity of a chemically inhomogeneous star with good accuracy by idealizing the inhomogeneity in terms of a discontinuous jump in composition, if we place the discontinuity so that the over-all composition remains unchanged.

TABLE 3*

COMPARISON OF CONTINUOUS AND DISCONTINUOUS MODELS

Model	log $C/t_c^{1/2}(\mu_e/\mu_m)^{7.7}$	log $(t_c\, \mu_e/\mu_m)$
I cont. model	−5.93	+0.30
I discont. compar.	−5.90	+0.30
II cont. model	−5.82	+0.44
II discont. compar.	−5.80	+0.54
III cont. model	−5.73	+0.56
III discont. compar.	−5.66	+0.87
IV cont. model	−5.70	+0.59
IV discont. compar.	−5.59	+1.02
V cont. model	−5.79	+0.40
VI cont. model	−5.34	+1.11
VII cont. model	−5.31	+1.13
VII discont. compar.	−5.20	+5.22
VIII cont. model	−5.66	+0.70
IX cont. model	−5.47	+0.95
IX discont. compar.	−5.45	+2.26
Cowling model	−5.97	−0.05

* For stars of the same mass, central temperature, and mean hydrogen content, but with different distributions of the hydrogen through the interior, luminosities and radii are proportional to the antilogs of the first and second tabulated quantities, respectively.

An even rougher idealization appears permitted if only an approximate value of the luminosity is needed. The last line of Table 3 gives the relevant material for the Cowling model, which has a completely homogeneous composition but is otherwise exactly equivalent to all the models here considered (Härm and Rogerson, 1955). Consider again stars with a given mass, central temperature, and over-all composition. Then the second column of Table 3 shows that all the inhomogeneous models give higher luminosities than the homogeneous Cowling model. The differences, in terms of bolometric magnitude, however, generally amount to less than 1 mag. and do not exceed 2 mag. even in the most extreme cases among the samples here considered. These differences—though not negligible in accurate computations—are only a moderate fraction of the 5–7 mag. by which the star will brighten up during its evolution because of the increase in over-all molecular weight caused by the nuclear transmutations. Thus one sees again that the luminosity of a star is greatly affected by the over-all composition (second bracket in eq. [26]) but depends relatively little on the distribution of the composition throughout the star, i.e., on the model (last bracket in eq. [26]), as was emphasized long ago by Eddington.

The last column of Table 3 gives the logarithm of the radius in its dependence on the model. Comparing, first, all the inhomogeneous models with the homogeneous Cowling model, one sees again the well-known effect that chemical inhomogeneities (with a mean molecular weight decreasing outward) tend to enlarge the stellar radius, often by big factors. A homogeneous model can obviously not be used to compute the radius of a distinctly inhomogeneous star.

Finally, one may compare in Table 3 the radii of the present models of continuously varying composition with those of the discontinuous models. It is seen that the simpler discontinuous models well represent the tendency of inhomogeneous stars to have increased radii; and even the amount of the increase is represented by the discontinuous models with some accuracy as long as this increase over the Cowling model is not more than a factor of 3. For the more extended stars, however, the discontinuous models appear to exaggerate the radius. In fact, for extreme cases like the present model VII, in which the inhomogeneity is spread over 70 per cent of the stellar mass, the equivalent discontinuous model cannot be used for the computation of the radius in any approximation.

In summarizing the results regarding the radius, one may conclude from the present sample of models that the radius of a star depends delicately on the variation of the chemical composition throughout the star, i.e., on the model (third bracket of eq. [27]), while it depends only moderately on the over-all composition (second bracket of eq. [27]). This has two consequences. First, the observed radius of the star can be used for the determination of the over-all composition of the star only if the star is sufficiently young that the nuclear processes cannot yet have produced large inhomogeneities. Second, for inhomogeneous stars the variation of the composition throughout the interior has to be determined in fair detail by considerations of the evolution, before the radius can be computed with sufficient accuracy to warrant comparison with observed radii or effective temperatures.

REFERENCES

Comrie, L. J. 1932, *British A. Adv. Sci. Math Tables*, Vol. 2.
Härm, R., and Rogerson, J. 1955, *Ap. J.*, **121**, 439.
Oke, J. B., and Schwarzschild, M. 1952, *Ap. J.*, **116**, 317.
Wares, G. W., and Chandrasekhar, S. 1949, *Ap. J.*, **109**, 551.